Desalination and Water Treatment
www.deswater.com

doi: 10.5004/dwt.2017.20150

63 (2017) 103–112
February

Chromium(VI) removal by tri-n-octylamine/n-heptane via a pseudo-emulsion-based hollow fiber strip dispersion technique

Yuchen Wang[a], Yingxue Li[b,*], Yijian Zhong[c], Chongwei Cui[a,*]

[a]*School of Municipal and Environmental Engineering, Harbin Institute of Technology, Harbin, China, Tel. +86 18845181188; email: cuichongwei1991@126.com (C. Cui), Tel. +86 13654686578; email: wyc19890714@yeah.net (Y. Wang)*
[b]*Institute of Pharmaceutical and Environmental Engineering, Changzhou Vocational Institute of Engineering, Changzhou, China, Tel. +86 15846593402; email: yingxue1213@163.com*
[c]*College of Environmental Science and Engineering, Guilin University of Technology, Guilin, China, Tel. +86 18845181188; email: hitzhongyijian@vip.qq.com*

Received 21 March 2016; Accepted 10 August 2016

ABSTRACT

Transport of Cr(VI) from acidic media via a pseudo-emulsion-based hollow fiber strip dispersion (PEHFSD) technique using tri-n-octylamine (N235) dissolved in n-heptane was investigated. The effects of various hydrodynamic and chemical parameters, including the flow rates, variation in feed pH, initial Cr(VI) concentration, and N235 concentration in the pseudo-emulsion, on Cr(VI) permeation were analyzed. The optimum conditions for Cr(VI) separation from hydrochloric acidic media were also estimated. The analysis of Cr(VI) transport was made on the basis of the overall mass-transfer coefficient of permeation; the resistances of mass transfer were also evaluated. The results indicated that the ion transport is controlled by the diffusion of Cr(VI) species in the stagnant film between the aqueous solution and the membrane liquid.

Keywords: Chromium(VI); N235; Pseudo-emulsion-based hollow fiber strip dispersion; Liquid membrane; Mass-transfer

1. Introduction

Cr is a lustrous, silver-gray metal. It exists in all oxidation states from 0 to VI, and its stable oxidation states are +III and +VI. Cr(VI) has been long identified as a carcinogen and teratogen based on its chemical properties. Unlike Cr(VI), Cr(III) is an essential element and does not pose a significant carcinogenic risk. The World Health Organization (WHO) and U.S. Environmental Protection Agency (USEPA) have classified Cr(VI) as an immense threat to aquatic ecosystems and a human carcinogen. Indeed, the discharge of industrially produced Cr waste liquid associated with ore refining, electroplating, wood preservatives, leather tanneries, metallurgy, and chrome pigments contaminates aquatic ecosystems and has led to an ecological security crisis [1,2]. Therefore, it is imperative to exploit new technologies to eliminate this contamination and reuse waste materials, given the current grievous ecological crisis and resource shortage.

The maximum discharge of Cr(VI) to surface water is limited to 0.05 mg·L^{-1} by the USEPA [3,4]. Given this strict regulation, the interest in Cr removal and reuse has increased rapidly over the last decade. Various methods, such as reduction, solvent extraction, ion exchange, cementation, electrochemical precipitation, ultrafiltration, biosorption, electrodialysis, and membrane separation, have been adopted to remove Cr(VI) from industrial effluents. Among these, liquid membrane separation is a promising technique. The liquid membrane pertraction technique combines solvent extraction and re-extraction into a single step, and is a dynamically non-equilibrium diffusion process governed by the kinetics of membrane transport. These technologies are being increasingly utilized for ion separation because

* Corresponding author.

liquid membranes do not suffer from the shortcomings of traditional solvent extraction methods such as solvent loss, and emulsion formation. Among them, liquid membrane configurations like supported liquid membrane (SLM) have the potential for large-scale application. Briefly, in a SLM, an organic solvent is immobilized in the pores of a hydrophobic porous polymer or an inorganic support material by capillary forces [5]. Hollow fiber contactors designed on a basis of SLM technique are known as hollow fiber SLM (HFSLM), which can provide large surface area per volume and high mass-transfer rate. Although they have numerous drawbacks such as lack in stability during long-term operation, liquid membrane technologies are increasing used to separate heavy and toxic metals from diluted solutions [6–18]. Thus, modifications and improvements are needed.

To improve the stability of HFSLM, the latest smart techniques for strip/organic dispersion methodologies, such as pseudo-emulsion-based hollow fiber strip dispersion (PEHFSD), are widely applied in separation because they combine the advantages of emulsion liquid membranes and non-dispersion solvent extraction [19–26]. The PEHFSD technique gives improved stability during device operation [27–30]. However, the data available on ion separation using commercially available hydrophobic hollow fiber modules are scarce. Thus, to evaluate the potential use of PEHFSD for ion separation, a reaction device designed with commercial materials was analyzed. Additionally, a bridge (carrier) for Cr(VI) transport in organic solvent must be established based on the liquid membrane design. N235 is an economical straight-chain tri-n-octylamine and can react with metallic anions through anion exchange and thus achieve the goal of separation [31,32]. However, observations of the extraction equilibrium of Cr(VI) using N235 are scarce.

The objective of this study is to utilize a reaction device designed with polyvinylidene fluoride hollow fiber membrane to evaluate the transport properties of Cr(VI) via a dispersion liquid membrane technique, and to explore the facilitated transport of Cr(VI) by N235. A permeation model describing the transport mechanism was used to evaluate the mass-transfer resistances.

2. Experimental

2.1. Materials

N235, a light yellow oily liquid (25°C), is a tertiary amine with alkyl chains linked to nitrogen atoms, and was obtained from the Shaoyang Institute of Chemical Industry (Hunan, China). This tertiary amine can react with acid to form ammonium salts. Analytical grade n-heptane was used as the diluent. A stock solution of Cr(VI) was prepared from solid $K_2Cr_2O_7$. All other chemicals used were of analytical reagent grade.

2.2. Experimental procedure

The Cr(VI) removal achieved via the PEHFSD technique was studied using a polyvinylidene fluoride microporous tubular hydrophobic membrane purchased from the Institute of Biological and Chemical Engineering of Tianjin Polytechnic University (Tianjin, China). The module details and hollow fiber membrane characteristics are given in Table 1.

Table 1
Characteristics of the hollow fiber module

Characteristic	Value
No. of fibers	100
Polymeric material	Polyvinylidene fluoride
Active contact area	0.05 m^2
Fiber inner diameter (d_i)	0.8 mm
Fiber outer diameter (d_o)	1.15 mm
Fiber thickness (d_{org})	0.15~0.18 mm
Fiber length (L)	22 cm
Porosity (ε)	82%~85%
Pore size	0.16 μm
Tortuosity (τ)	1.2

The strip dispersion technology involved a unique membrane module for extraction and re-extraction, and the setup used for the metal separation consisted of a peristaltic pump and a gear pump. The waste liquid containing the target species circulated in the tube side of the liquid membrane device, and a magnetic stirrer was used to homogenize the solution; NaOH solution (stripping agent) was dispersed in the organic membrane solution in a tank with an impeller stirrer to form the dispersion solution. The strip dispersion solution then circulated in the shell side from the reservoirs to the membrane module to provide a continuous supply of the organic solution to the membrane pores, and form a stable liquid membrane supported in the pores. The organic solution was able to wet the microporous wall of the fiber because of its hydrophobic nature. The interface was maintained in the pore by applying a higher pressure to the aqueous phase than to the dispersion phase. The differential pressure was always kept below the breakthrough pressure. Besides, after the mixing was stopped, clear and fast phase separation of the pseudo-emulsion solution was observed. PEHFSD was conducted by passing the Cr(VI) solution through the tube side and the pseudo-emulsion through the shell side in counter-current mode. The pseudo-emulsion phase was a solution (400 cm^3) containing 200 cm^3 of 1.0% v/v (0.02 $mol \cdot L^{-1}$) N235/n-heptane and 200 cm^3 of 1.0 $mol \cdot L^{-1}$ NaOH, and 1,000 cm^3 of 0.01 $g \cdot L^{-1}$ Cr(VI) simulated hydrochloride waste liquid (pH = 1.0) was prepared by appropriately diluting the stock solution. The flow rates of the feed phase and pseudo-emulsion phase in the module were 100 and 80 $cm^3 \cdot min^{-1}$, respectively, unless otherwise stated. The transmembrane pressure (TMP) was maintained at 20 kPa. The optimum stirring rate in the dispersion solution was 120 rpm. All experiments were conducted at room temperature.

At predetermined times, small aliquots of the aqueous solutions were collected, and their Cr concentrations were analyzed by inductively coupled plasma (ICP) spectroscopy (Perkin Elmer Optima·5300DV spectrophotometer). All the experiment runs were carried out in duplicate and took the average.

3. Results and discussion

A schematic of the transfer of Cr(VI) by PEHFSD with N235 is displayed in Fig. 1. Extraction mechanism of tertiary

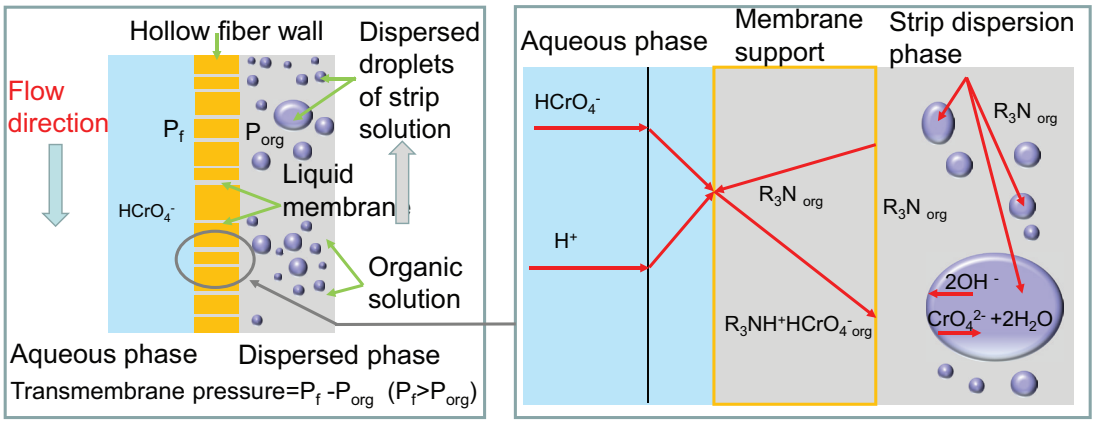

Fig. 1. Schematic of transport mechanism of Cr(VI) ions in PEHFSD.

amine is that the basic nitrogen atom can react with variety of inorganic and organic acids to form amine salts and then amine salts react with metallic anion by anion exchange to achieve the goal of separation [33]. 0.01 g·L^{-1} Cr(VI) ions in acidic media (pH = 1.0) existed as $HCrO_4^-$ [1,2], and reacted with the protonated carriers via an anion-exchange reaction, as described by Eq. (1). The extracted complexes then diffused through the pores of the hollow fibers toward the membrane-pseudo-emulsion interface, where Cr(VI) was stripped from the loaded organic solution in the interface of organic-strip drop (Eq. (2)). In these equations, the subscripts f and org refer to the feed and organic phases, respectively.

$$R_3NHCl_{(org)} + HCrO_{4(f)}^- \Leftrightarrow [(R_3NH)\cdot HCrO_4]_{(org)} + Cl^-_{(f)} \quad (1)$$

$$[(R_3NH)\cdot HCrO_4]_{(org)} + 2NaOH_{(f)} \Leftrightarrow R_3N_{(org)} + Na_2CrO_{4(f)} + 2H_2O_{(f)} \quad (2)$$

The extraction equilibrium and equilibrium constant can be described with the following equation:

$$K_{ex} = \frac{[(R_3NH)HCrO_4][Cl^-]}{[R_3NHCl][HCrO_4^-]} \quad (3)$$

Thus, the distribution coefficient can be expressed as follows:

$$\log D = \log K_{ex} + \log[R_3NHCl] - \log[Cl^-] \quad (4)$$

To evaluate the influence of various operating conditions on ions permeation, the transport of Cr(VI) via the PEHFSD technique was investigated. This analysis was performed based on the overall mass-transfer coefficient of Cr(VI) permeation. The observations showed that the overall mass-transfer coefficients can be calculated using the equations derived from the simplified and rigorous models [34–37].

Considering the linear concentration gradient and the absence of back-mixing, the calculation method of overall permeability coefficient derived from the simplified model is shown in Eq. (5), whereas that derived from the rigorous model for the transport of Cr(VI) in PEHFSD operating in recycling mode is shown in Eq. (7); the overall permeability coefficient can be calculated from the data of S shown in Eq. (6) [20]:

$$\ln\left(\frac{c_t}{c_0}\right) = -\frac{A}{V_f}P_{Cr}t \quad (5)$$

where A is the contact area; P is the overall permeability coefficient.

$$V_f \ln\left(\frac{[Cr]^T_{f,t=0}}{[Cr]_f}\right) = St \quad (6)$$

where S is the slope of the linear relationship of the fiber and module geometries, the linear velocity of the solutions, and the overall permeability of the system.

$$P'_{Cr} = -\frac{u_f r_i}{2L}\ln\left[1-\left(\frac{S}{Q_f}\right)\right] \quad (7)$$

where L is the fiber length; Q is the flow rate; u is the linear velocity and V is the volume.

When deriving the overall mass-transfer coefficient model, it was assumed that the resistance of the chemical reaction can be ignored and that the ion diffusion in the liquid membrane and the boundary layers on both sides of the membrane can be described by Fick's law.

The design of HFSLM modules for the separation of solute using the overall permeability coefficient P centers on three mass-transfer resistances. One occurs in the liquid flowing through the hollow fiber lumen. The second resistance corresponds to the solute-complex diffusion across the liquid membrane on the porous wall of the fiber. Finally, the third one is the aqueous interface created on the outside of the fiber. Eq. (8) is the overall mass-transfer resistance based on the resistance in series approach that takes into account the resistance in the feed boundary layer (tube side), the

resistance in the membrane and the resistance in the outer aqueous interface, which is reported elsewhere [7,20]. The reciprocal of the overall permeability coefficient P can be related to the various mass-transfer resistances as follows:

$$\frac{1}{P}=\frac{1}{k_i}+\frac{r_i}{r_{lm}}\frac{1}{Dk_m}+\frac{r_i}{r_o}\frac{1}{k_o} \tag{8}$$

where r_i, r_o and r_{lm} are the inner, and outer radii of the hollow fiber and the hollow fiber log-mean radius, respectively. k_i and k_o are the interfacial coefficients corresponding to the inner and outer aqueous boundary layers. The membrane permeability is denoted by P_m, which is related to the distribution coefficient of Cr(VI) with N235 by:

$$P_m = Dk_m = k_m K_{ex}[R_3NH^+Cl^-]_{org}[Cl^-]_f^{-1} \tag{9}$$

Inserting Eq. (9) into Eq. (8) gives:

$$\frac{1}{P}=\frac{1}{k_i}+\frac{r_i}{r_{lm}}\times\frac{[Cl^-]_f}{k_m K_{ex}[R_3NH^+Cl^-]_{org}}+\frac{r_i}{r_o}\times\frac{1}{k_o} \tag{10}$$

When the chemical reaction is instantaneous on the pseudo-emulsion side, the contribution of the outer aqueous interface can be excluded from Eq. (10), and the overall permeability coefficient is given by:

$$\frac{1}{P}=\frac{1}{k_i}+\frac{r_i}{r_{lm}}\cdot\frac{[Cl^-]_f}{k_m K_{ex}[R_3NH^+Cl^-]_{org}} \tag{11}$$

3.1. Influence of the active contact area on Cr(VI) permeation

The influence of the module's active contact area on Cr(VI) permeation was explored. The results are shown in Fig. 2. The metal permeation was observed to increase as the interfacial area increased because an increase in the interfacial area represents an increase in the reaction space; the reason is that the mass-transfer process is mainly controlled by diffusion. Thus, the decrease of contact area can increase the mass-transfer resistance, and then decrease the permeability of metal ions. The results were fitted to Eqs. (5) and (6), plotting $\ln(C_0/C_t)$ against time gave a straight line. This behavior could be explained by mass modeling. However, increasing the module's interfacial area would also increase its cost. Because the price of membrane materials with an area higher than 0.05 m^2 is twice of the membrane materials with an area lower than 0.05 m^2. Thus, the economic benefits were analyzed, and Fig. 2 shows that the module with an interfacial area of 0.05 m^2 was suitable for ion separation.

3.2. Influence of the operation mode on Cr(VI) permeation

To optimize the transport of the target species on the tube side, the influence of the operation mode between the lumen and shell side on Cr(VI) permeation was explored. The results are described in Fig. 3. The countercurrent between the tube side and the shell side facilitates Cr(VI) transport by increasing the ion collisions and complex strength. The permeability coefficients were calculated to be 9.1×10^{-4} and 9.6×10^{-4} cm·s^{-1} using Eqs. (5) and (7), respectively. Thus, the countercurrent is suitable for ion separation.

3.3. Influence of the feed phase and pseudo-emulsion phase flow rates

The influence of the flow rates on the tube and shell sides was investigated to optimize Cr(VI) transport. The results are described in Figs. 4 and 5.

Fig. 4 indicated that the permeability coefficient increased as the flow rate increased (60–100 cm^3·min^{-1}) on the lumen side because the higher shear force resulting from the higher lumen side flow rate enhanced the liquid membrane's renewal rate and lead to a thinner liquid membrane layer, thereby greatly reducing the individual mass-transfer resistance on the lumen side. However, P also decreased

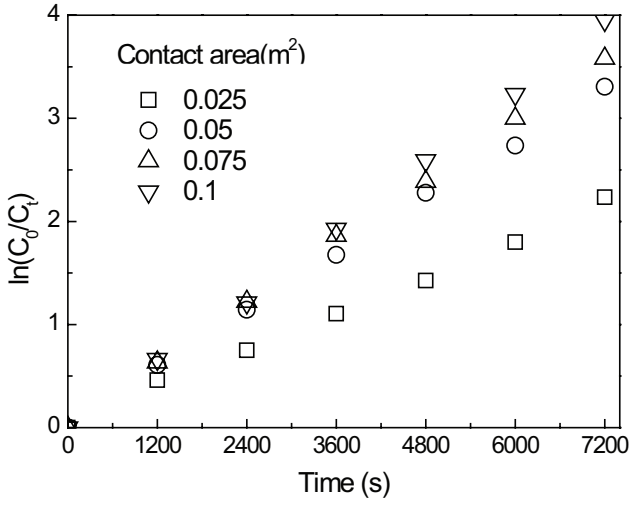

Fig. 2. Influence of the contact area on Cr(VI) permeation as a function of time in recycling mode.

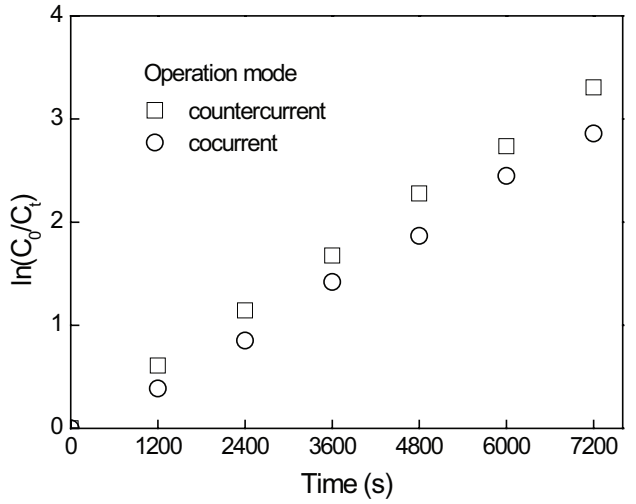

Fig. 3. Influence of the module's operation mode on Cr(VI) permeation as a function of time in recycling mode.

because of the lower residence time at higher flow rates (120 $cm^3 \cdot min^{-1}$), which provides insufficient time for the Cr(VI)-N235 complex to form. In addition, high flow rates create greater turbulence in the aqueous phase, which forces the organic phase out of the micropores and makes it difficult to maintain the interface; this turbulence also alters the thickness of the boundary layers of the interface. Thus, to avoid contamination of the aqueous phase by the pseudo emulsion that occurs at the high flow rates, a flow rate of 100 $cm^3\ min^{-1}$ was used for further investigations.

Fig. 5 shows that the variation trend of the $\ln(C_0/C_t)$ is also increased first and then decreased because the dissociative reaction is related to the disturbance of the liquid flow on the shell side. A flow rate of 80 $cm^3 \cdot min^{-1}$ should thus be used in the dispersion solution.

3.4. Influence of TMP

The loaded organic solution supported at the interface of the liquid membrane boundary will leak into the tube side when no TMP exists between the tube and shell sides. The leakage will decrease Cr(VI) permeation due to the loss of the liquid membrane. Thus, the influence of the TMP on Cr(VI) transport was explored. The results are shown in Fig. 6.

The results showed that liquid membrane leakage could be avoided with the TMP of 20 kPa between the tube side and the shell side. However, the permeability coefficient decreases with TMP increase because of the leakage of membrane solution from the micropores. The permeability is controlled by diffusion, and thus a plot of $\ln(C_0/C_t)$ vs. time gives a straight line. The overall mass-transfer coefficient can then be calculated from the slope of the linear plot.

3.5. Influence of N235 concentration

The N235 serves as the carrier for ion transport. Thus, the influence of the N235 concentration in the pseudo-emulsion in recycling mode was evaluated. No transport of Cr(VI) occurred in the absence of N235. Plots of $\ln(C_0/C_t)$ vs. time for different carrier amounts are illustrated in Fig. 7. In the linear

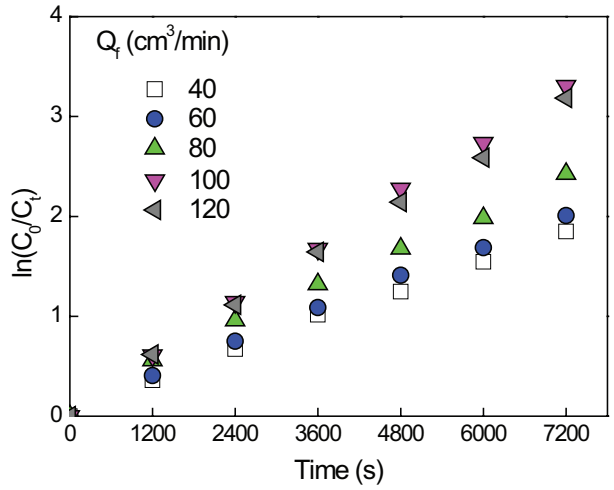

Fig. 4. Influence of the feed phase flow rate on Cr(VI) permeation as a function of time in recycling mode.

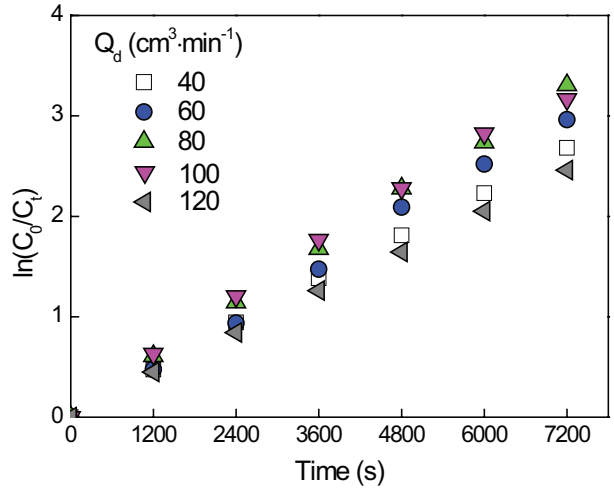

Fig. 5. Influence of the pseudo-emulsion phase flow rates on Cr(VI) permeation as a function of time in recycling mode.

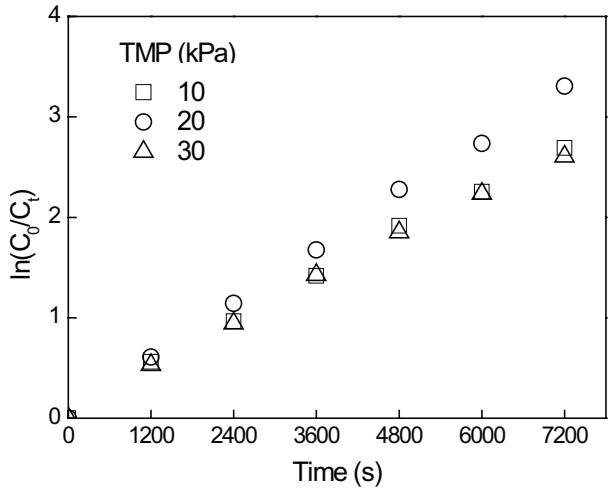

Fig. 6. Influence of TMP on Cr(VI) permeation as a function of time in recycle mode.

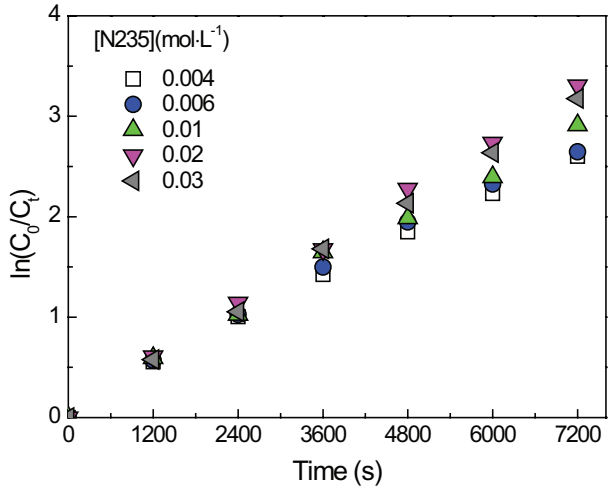

Fig. 7. Influence of N235 concentration on Cr(VI) permeation as a function of time in recycling mode.

region, the slopes are related to a mass-transfer coefficient. The results indicated that Cr(VI) permeation increased as the concentration of N235 increased to 0.02 mol·L^{-1}; therefore, the transport rate is limited by diffusion through the aqueous film. Furthermore, the limiting permeability was calculated by assuming that diffusion in the fibers is negligible and that the permeation process is controlled by diffusion in the stagnant film of the aqueous phase, as shown in Eq. (12):

$$P_{\lim} = \frac{D_f}{d_f} \tag{12}$$

where D_f is the aqueous diffusion coefficient of the Cr(VI) species (1.76×10^{-5} cm^2·s^{-1} [23,24]), and the values of $P_{\lim}$ were calculated to be 9.1×10^{-4} and 9.6×10^{-4} cm·s^{-1} with Eqs. (5) and (7), respectively. Thus, the thicknesses of the aqueous film (d_f) calculated using Eq. (12) were approximately 1.9×10^{-2} and 1.8×10^{-2} cm, respectively. These values are considered to be the minimum thickness of the aqueous diffusion layer.

3.6. Influence of pH

The metal ions loaded on carriers diffuse into the liquid membrane and dissociate onto the interface of the membrane-pseudo-emulsion boundary;, then, they become enriched in the strip dispersion phase, and the types of species present depend on the pH value of the aqueous solution. Based on observations of solvent extraction, the distribution coefficient for Cr(VI) separation was suitable at pH 0.5–1.0 [33]. Thus, the influence of pH in strongly acidic media on Cr(VI) permeation was investigated. The results are displayed in Fig. 8. Varying the pH value (0.5–1.0) of the aqueous solution was found to exert no significant influence on metal permeation and resulted in very similar *P* values. Plotting $\ln(C_0/C_t)$ vs. time gives a straight line, and the overall mass-transfer coefficient can be calculated from the slope of the linear plot using Eqs. (5) and (7). In contrast, plotting $\ln(C_0/C_t)$ vs. time gives a curve line at a pH value of 1.5, and in this case, the mass-transfer model is not suitable for the evaluation of the permeability coefficients. The species that existed in acidic solution (pH = 1.0) is identified as $HCrO_4^-$.

3.7. Influence of initial metal ion concentration

The influence of the metal ion concentration on permeability was also investigated due to the target ions are driven to transport from hydrophilic to hydrophobic zone on the gradient surface. The results are shown in Fig. 9. It is indicated that hexavalent chromium species transport through the liquid membrane is increased as the initial metal concentration decreases. The reason is that the permeability is mainly controlled by diffusion of metal species; the increase of metal amounts could lead to the competition of the limited complexation site and increase the ions diffusion resistance; thus, the transport rate decreases. However, in the presence of high abundances of the metal species, the decreased transport rate could be recovered by either increasing the surface areas of the membrane or prolonging the operation time.

3.8. Influence of the NaOH concentration

The transport of metal ions in liquid membranes occurs via the diffusion of the complexes along the density gradient. The presence of OH^- could influence the diffusion rate and the regeneration of the liquid membrane and, thus, alter the metal permeation. Therefore, the influence of NaOH on Cr(VI) permeation was evaluated (Fig. 10). The metal permeation was observed to increase as the concentration of OH^- increased. OH^- acts as the driving force of mass-transfer and liquid membrane regeneration. Increasing the OH^- concentration benefits the dissociation of loaded complexes and, thus, improves mass transfer. The recovery rate of chromium(VI) is more than 92% with 1.0 M NaOH as the strippant and the regenerated solvent could be reused in succeeding separation and recovery of chromium(VI), which we have reported elsewhere [38].

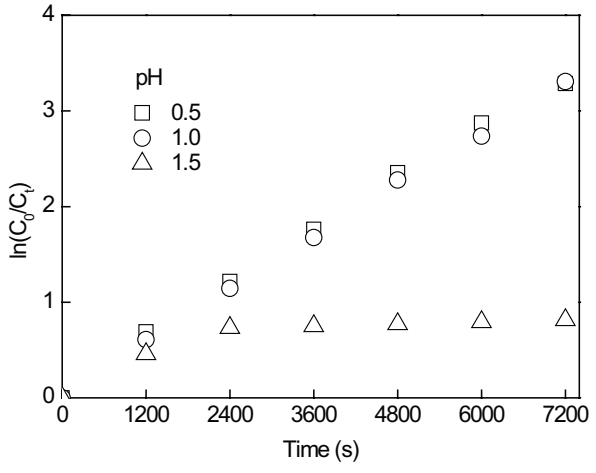

Fig. 8. Influence of the pH value on Cr(VI) permeation as a function of time in recycling mode.

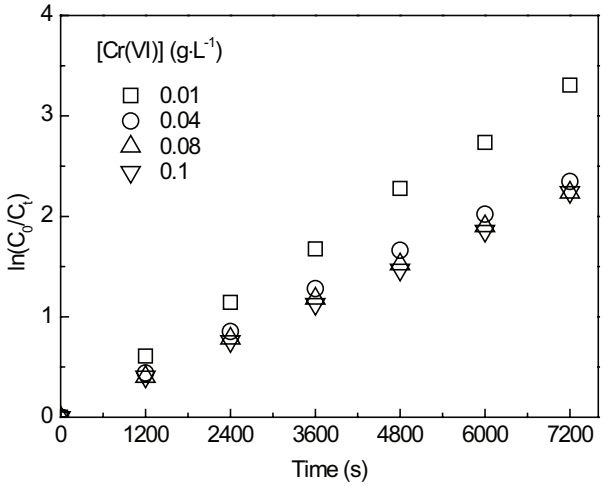

Fig. 9. Influence of the initial Cr(VI) concentration on permeation as a function of time in recycling mode.

3.9. Ions transport using various hollow fiber module operational modes: a comparison

The transport of Cr(VI) with N235 diluted in n-heptane as liquid membrane was explored using different technologies such as HFSLM and PEHFSD. Fig. 11 shows that the maximum permeability was achieved using PEHFSD in countercurrent mode, although this method was applied by dispersing the organic phase into the strip solution. The P values for ions separation with PEHFSD were calculated to be 9.1 × 10^{-4} and 9.6 × 10^{-4} cm·s^{-1} using Eqs. (5) and (7), respectively. In contrast, the P values for ion separation with HFSLM were about 5.8 × 10^{-4} cm·s^{-1} using Eqs. (5) and (7), respectively. The operation of PEHFSD was also observed to be stable. Thus, this technique is a promising alternative to traditional methods.

3.10. Estimation of the mass-transfer coefficients

Eq. (11) indicates that the local value of the total resistance is the sum of the mass-transfer resistances inside the fiber and across the fiber wall. The overall permeation coefficient is a function of the individual transfer coefficients k_i and k_m (Eq. (11)). The mass-transfer coefficient on the tube side (k_i) with laminar flow and the membrane mass-transfer coefficient (k_m) can be calculated based on empirical correlations. The k_i and k_m can be calculated using Eqs. (13) and (14) [20]:

$$k_i = 1.64\frac{D_f}{d_i}\left(\frac{d_i^2 \times u}{L \times D_f}\right)^{\frac{1}{3}} \quad (13)$$

$$k_m = \frac{D_m \varepsilon}{\tau(d_o - d_i/2)} \quad (14)$$

where D_f and D_m are the diffusion coefficients of Cr(VI) ions in the solution and the Cr(VI) complex in the membrane, respectively. D_f and D_m can be estimated using the Wilke–Chang correlation [26] as shown in Eq. (15). d_o and d_i are the outer and inner diameters of the hollow fiber (cm), respectively. u is the linear velocity of the feed solution on the tube side (cm·s^{-1}); ε is the porosity of the hollow fibers and τ is tortuosity of the hollow fibers.

$$D_{AB} = 7.4 \times 10^{-15}\frac{(\varphi M_B)^{\frac{1}{2}}T}{\eta V_A^{0.6}} \quad (15)$$

where φ is the solvent association coefficient; M is the molecular weight of the solvent (g·mol^{-1}); T is the temperature (K); η is the dynamic viscosity of the solvent (Pa·s) and V_A is the molecular size of the solute at the normal boiling point (cm^3·mol^{-1}). Therefore, according to the Wilke–Chang correlation (Eq. (15)), the estimated diffusivity of chromic acid was approximately 1.76 × 10^{-5} cm^2·s^{-1}, as observed by Ho and Poddar [23] and Bringas et al. [24], whereas the diffusion coefficient of the Cr complex in the membrane (0.02 mol·L^{-1} N235 diluted in n-heptane) calculated from Eq. (15) was approximately 6.72 × 10^{-6} cm^2·s^{-1}. Thus, the values of k_i and k_m were estimated to be 1.37 × 10^{-3} and 6.12 × 10^{-5} cm·s^{-1}, respectively, and the resistances on the tube side and in the membrane were 729 and 253 s·cm^{-1}, respectively.

The calculated value of the effective diffusion coefficient of the Cr(VI) complex through the organic membrane solution is defined as follows:

$$D_{eff} = k_m \tau d_{org} \quad (16)$$

where d_{org} is the membrane thickness. Then, D_{eff} can be estimated as 1.20 × 10^{-6} cm·s^{-1}.

In addition, Eq. (11) was used to evaluate k_i, k_m, and the diffusivity. By plotting 1/P as a function of $[Cl^-]_i/K_{ex}[R_3NH^+Cl^-]_{org}$ in acidic medium (0.1 M HCl), a straight line with a slope of $r_i/r_{lm}\cdot k_m$ and an ordinate that can be calculated (Fig. 12).

The k_i and k_m calculated using the simplified model reported by Danesi [34] were 1.19 × 10^{-3} and 5.64 × 10^{-5} cm·s^{-1}, respectively. Thus, the D_{eff} was calculated to be 1.22 × 10^{-6} cm·s^{-1}. The first term calculated from the simplified

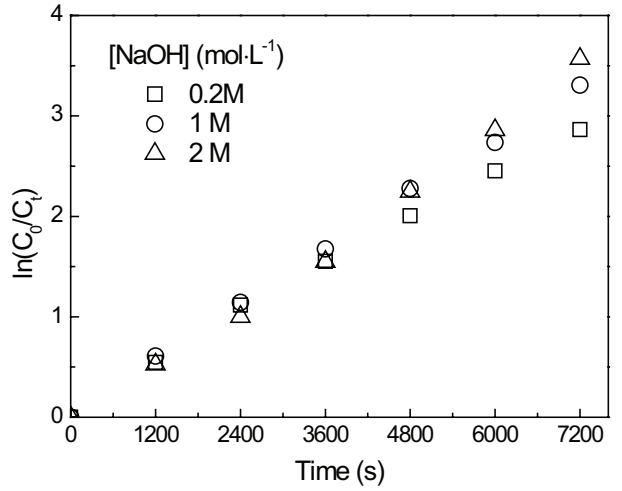

Fig. 10. Influence of NaOH concentration on Cr(VI) permeation as a function of time in recycling mode.

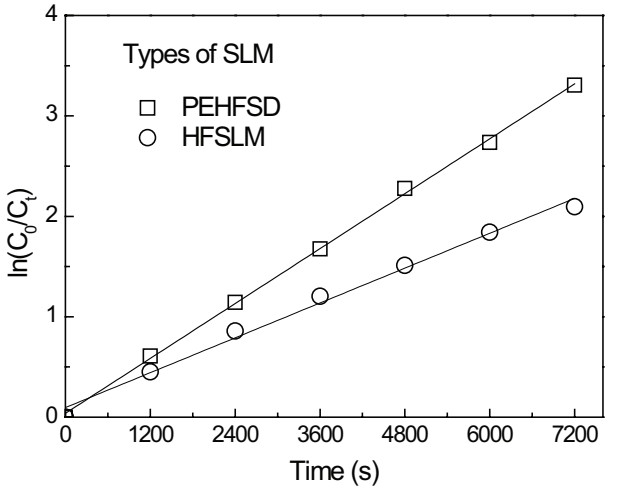

Fig. 11. The permeability of Cr(VI) in various hollow fiber module as a function of time in recycling mode.

model was reciprocal of k_i (838 s·cm^{-1}), whereas the second term of the equation ranged from 2.75×10^2 to 5.67×10^2 s·cm^{-1}.

The k_i and k_m values calculated from the rigorous model were 1.34×10^{-3} and 5.10×10^{-5} cm·s^{-1}, respectively. Thus, the D_{eff} was 1.00×10^{-6} cm·s^{-1}. The first term calculated from the rigorous model was the reciprocal of k'_i (745 s·cm^{-1}), whereas the second terms of the equation ranged from 3.04×10^2 to 6.27×10^2 s·cm^{-1}.

Tables 2 and 3 show that the membrane diffusion resistance becomes dominant as the concentration of the extractant in the organic solution decreases. In addition, the fractional resistance of each step in the overall process (R_i^0 and R_m^0) can be calculated as follows:

$$R_i^0 = \frac{R_i}{R_i + R_m} \tag{17}$$

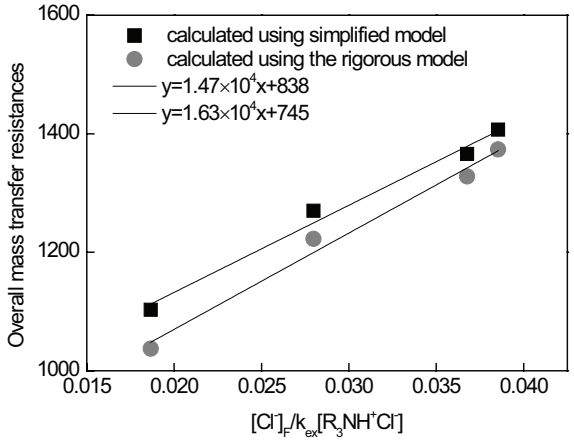

Fig. 12. Plot of $1/P$ as a function of $[Cl^-]_f/K_{ex}[R_3NH^+Cl^-]$.

$$R_m^0 = \frac{R_m}{R_i + R_m} \tag{18}$$

where R_i and R_m are the mass-transfer resistances on the tube side and in the membrane, respectively. The results indicated that the ions transport was controlled by the diffusion of Cr(VI) species in the stagnant film between the aqueous solution and the membrane liquid. The contributions of the interfacial resistances associated with the extraction and re-extraction reactions can be ignored. This model was confirmed to be valid, and very good agreement between the experimental and theoretical data was achieved.

4. Conclusions

The PEHFSD technique was used to transport of Cr(VI) with N235. The overall mass-transfer coefficient results indicated that the aqueous and membrane mass-transfer resistances were dominant compared with the overall mass-transfer resistances. The diffusional parameters, including the rate controlling steps, were evaluated. The theoretical values of k_i, k_m and D_{eff} with 0.02 mol·L^{-1} N235 in an organic solvent calculated based on the Wilke–Chang correlation were 1.37×10^{-3}, 6.12×10^{-5} and 1.20×10^{-6} cm·s^{-1}, respectively. The experimentally determined values of k_i, k_m and D_{eff} calculated based on the simplified model were 1.19×10^{-3}, 5.64×10^{-5} and 1.22×10^{-6} cm·s^{-1}, respectively. The resistances on the tube side and in the membrane were estimated to be 838 and (2.75–5.67) $\times 10^2$ s·cm^{-1}, respectively. Whereas k_i, k_m and D_{eff} calculated based on the rigorous model were 1.34×10^{-3}, 5.10×10^{-5} and 1.00×10^{-6} cm·s^{-1}, respectively. The resistances on the tube side and in the membrane were estimated to be 745 and (3.04–6.27) $\times 10^2$ s·cm^{-1}, respectively. The findings mentioned above indicate that the model is valid, and very good agreement between the experimental and theoretical data was achieved, which means this technique is a promising alternative to traditional methods.

Table 2

Mass-transfer resistances on the tube side and in the membrane calculated using the simplified model

[N235] (mol·L^{-1})	$1/P_{Cr}$ (s·cm^{-1}), exp	$1/k_i$ (s·cm^{-1})	$r_i[Cl^-]_f/r_{lm}k_mk_{ex}[R_3NH^+Cl^-]_{org}$ (s·cm^{-1})	$1/P_{Cr}$ (s·cm^{-1}), Eq. (11)	% R_i^0	% R_m^0
0.004	1,407	838	567	1,405	59.7	40.3
0.006	1,366		540	1,378	61.0	39.0
0.01	1,269		412	1,250	67.0	33.0
0.02	1,103		275	1,113	75.3	24.7

Table 3
Mass-transfer resistances on the tube side and in the membrane calculated using the rigorous model

[N235] (mol·L^{-1})	$1/P'_{Cr}$ (s·cm^{-1}), exp	$1/k'_i$ (s·cm^{-1})	$r'_i[Cl^-]_f/r'_{lm}k'_mk'_{ex}[R_3NH^+Cl^-]_{org}$ (s·cm^{-1})	$1/P'_{Cr}$ (s·cm^{-1}), Eq. (11)	% R'^0_i	% R'^0_m
0.004	1,374	745	627	1,372	54.3	45.7
0.006	1,328		598	1,343	55.5	44.5
0.01	1,223		456	1,201	62.0	38.0
0.02	1,037		304	1,049	71.0	29.0

Acknowledgment

This study was funded by the Commonweal Project of the Environmental Protection Agency through Grant Number 201209048.

Symbols

d_i — Internal diameter, mm
d_o — Outer diameter, mm
d_{org} — Fiber thickness, mm
L — Fiber length, cm
ε — Membrane porosity, μm
τ — Membrane tortuosity
P — Overall permeability coefficient, cm·s^{-1}
Q — Flow rate, cm^3·min^{-1}
u — Linear velocity, cm·s^{-1}
V — Volume, L
r_i — Inner radii of the hollow fiber, mm
r_o — Outer radii of the hollow fiber, mm
r_{lm} — Hollow fiber log-mean radius
k_i — Mass-transfer coefficients in the tube side, cm·s^{-1}
k_m — Membrane mass-transfer coefficients, cm·s^{-1}
P_m — Membrane permeability, m·s^{-1}
D_f — Diffusion coefficient in tube side, cm^2·s^{-1}
D_m — Membrane diffusion coefficient, cm^2·s^{-1}
φ — Solvent association coefficient
M — Molecular weight of solvent, g·mol^{-1}
T — Temperature, K
η — Dynamic viscosity of the solvent, Pa·s
V_A — Molecular size of solute at normal boiling point, cm^3·mol^{-1}
R_i — Mass-transfer resistances in the tube side, s·cm^{-1}
R_m — Mass-transfer resistances in the membrane, s·cm^{-1}

References

[1] K. Mukherjee, R. Saha, A. Ghosh, B. Saha, Chromium removal technologies, Res. Chem. Intermed., 39 (2013) 2267–2286.
[2] R. Saha, R. Nandi, B. Saha, Sources and toxicity of hexavalent chromium, J. Coord. Chem., 64 (2011) 1782–1806.
[3] P. Malaviya, A. Singh, Physicochemical technologies for remediation of chromium-containing waters and wastewaters, Crit. Rev. Environ. Sci. Technol., 41 (2011) 1111–1172.
[4] B. Saha, C. Orvig, Biosorbents for hexavalent chromium elimination from industrial and municipal effluents, Coord. Chem. Rev., 254 (2010) 2959–2972.
[5] V.S. Kislik, Liquid Membrane: Principles and Applications in Chemical Separations and Wastewater Treatment, Science Press, Beijing, 2010.
[6] S. Panja, R. Ruhela, A. Das, S.C. Tripathi, A.K. Singh, P.M. Gandhi, R.C. Hubli, Carrier mediated transport of Pd(II) from nitric acid medium using dithiodiglycolamide (DTDGA) across a supported liquid membrane (SLM), J. Membr. Sci., 449 (2014) 67–73.
[7] J.V. Sonawane, A.K. Pabby, A.M. Sastre, Pseudo-emulsion based hollow fiber strip dispersion: a novel methodology for gold recovery, AIChE J., 54 (2008) 521–525.
[8] P.V. Vernekar, Y.D. Jagdale, A.W. Patwardhan, A.V. Patwardhan, S.A. Ansari, P.K. Mohapatra, V.K. Manchanda, Transport of cobalt(II) through a hollow fiber supported liquid membrane containing di-(2-ethylhexyl) phosphoric acid (D2EHPA) as the carrier, Chem. Eng. Res. Des., 91 (2013) 141–157.
[9] I.B. Solangi, F. Ozcan, G. Arslan, M. Ersoz, Transportation of Cr(VI) through calix[4]arene based supported liquid membrane, Sep. Purif. Technol., 118 (2013) 470–478.
[10] Y.D. Jagdale, A.W. Patwardhan, K.A. Shah, S. Chaurasia, A.V. Patwardhan, S.A. Ansari, P.K. Mohapatra, Transport of strontium through a hollow fibre supported liquid membrane containing N,N,N′,N′-tetraoctyl diglycolamide as the carrier, Desalination, 325 (2013) 104–112.
[11] K. Chakrabarty, P. Saha, A.K. Ghoshal, Simultaneous separation of mercury and lignosulfonate from aqueous solution using supported liquid membrane, J. Membr. Sci., 346 (2010) 37–44.
[12] L.A. Santiago-Santiago, J.A. Reyes-Aguilera, M.P. Gonzalez, D. Cholico-Gonzalez, M. Avila-Rodriguez, Separation of Bi(III) and Sb(III) from Cu(II) HCl/H_2SO_4 mixed media by supported liquid membranes using cyanex 921 as carrier, Ind. Eng. Chem. Res., 51 (2012) 15184–15192.
[13] S.U. Rehman, G. Akhtar, M.A. Chaudry, K. Ali, N. Ullah, Transport of Ag^+ through tri-n-dodecylamine supported liquid membranes, J. Membr. Sci., 389 (2012) 287–293.
[14] S. Panja, P.K. Mohapatra, S.C. Tripathi, P.M. Gandhi, P. Janardan, Supported liquid membrane transport studies on Am(III), Pu(IV), U(VI) and Sr(II) using irradiated TODGA, J. Hazard. Mater., 237 (2012) 339–346.
[15] S. Panja, P.K. Mohapatra, S.C. Tripathi, V.K. Manchanda, Studies on uranium(VI) pertraction across a N,N,N′,N′-tetraoctyldiglycolamide (TODGA) supported liquid membrane, J. Membr. Sci., 337 (2009) 274–281.
[16] M. Aguilar, J.L. Cortina, Solvent Extraction and Liquid Membrane: Fundamentals and Application in New Materials, CRC Press, USA, 2007.
[17] L.J. Lozano, C. Godinez, A.P. de los Rios, F.J. Hernandez-Fernandez, S. Sanchez-Segado, F.J. Alguacil, Recent advances in supported ionic liquid membrane technology, J. Membr. Sci., 376 (2011) 1–14.
[18] N.M. Kocherginsky, Q. Yang, L. Seelam, Recent advances in supported liquid membrane technology, Sep. Purif. Technol., 53 (2007) 171–177.
[19] J.V. Sonawane, A.K. Pabby, A.M. Sastre, Pseudo-emulsion based hollow fibre strip dispersion (PEHFSD) technique for permeation of Cr(VI) using Cyanex-923 as carrier, J. Hazard. Mater., 174 (2010) 541–547.
[20] R. Gonzalez, A. Cerpa, F.J. Alguacil, Nickel(II) removal by mixtures of Acorga M5640 and DP8R in pseudo-emulsion based hollow fiber with strip dispersion technology, Chemosphere, 81 (2010) 1164–1169.
[21] F.J. Alguacil, M. Alonso, F.A. Lopez, A. Lopez-Delgado, I. Padilla, H. Tayibi, Pseudo-emulsion based hollow fiber with strip dispersion pertraction of iron(III) using $(PJMTH^+)_2(SO_4^{2-})$ ionic liquid as carrier, Chem. Eng. J., 157 (2010) 366–372.
[22] S. Agarwal, M.T.A. Reis, M.R.C. Ismael, J.M.R. Carvalho, Zinc extraction with Ionquest 801 using pseudo-emulsion based hollow fibre strip dispersion technique, Sep. Purif. Technol., 127 (2014) 149–156.
[23] W.S. W. Ho, T.K. Poddar, New membrane technology for removal and recovery of chromium from waste waters, Environ. Prog., 20 (2001) 44–52.
[24] E. Bringas, M.F. San Roman, I. Ortiz, Separation and recovery of anionic pollutants by the emulsion pertraction technology. Remediation of polluted groundwaters with Cr(VI), Ind. Eng. Chem. Res., 45 (2006) 4295–4303.
[25] W.S. W. Ho, Removal and Recovery of Radionuclides (e.g. Strontium) or Metals (e.g. Calcium) from Waste Water and Process Streams, Involves Using Combination of Supported Liquid Membrane and Strip Dispersion, US6328782-B1, 2001.
[26] C.R. Wilke, P. Chang, Correlation of diffusion coefficients in dilute solutions, AIChE J., 1 (1955) 264–270.
[27] A. Mondal, S. Ghosh, A. Bhowal, Vanadium extraction using pseudo-emulsion based hollow-fiber with strip dispersion technique, Sep. Sci. Technol., 48 (2013) 877–883.
[28] K.K. Sirkar, Membrane separation technologies: current developments, Chem. Eng. Commun., 157 (1997) 145–184.
[29] A.K. Pabby, A.M. Sastre, State-of-the-art review on hollow fibre contactor technology and membrane-based extraction processes, J. Membr. Sci., 430 (2013) 263–303.
[30] A.M. Sastre, A. Kumar, J.P. Shukla, R.K. Singh, Improved techniques in liquid membrane separations: an overview, Sep. Purif. Methods, 27 (1998) 213–298.

[31] X.M. Zhong, Y.H. Wu, Recovery of uranium and thorium from zirconium oxychloride by solvent extraction, J. Radioanal. Nucl. Chem., 292 (2012) 355–360.
[32] Z.N. Lou, Y. Xiong, J.J. Song, W.J. Shan, G.X. Han, Z.Q. Xing, Y.X. Kong, Kinetics and mechanism of Re(VII) extraction and separation from Mo(VI) with trialkyl amine, Trans. Nonferrous Met. Soc. China, 20 (2010) s10–s14.
[33] Y.X. Li, C.W. Cui, X. Ren, Y. Li, Solvent extraction of chromium(VI) from hydrochloric acid solution with trialkylamine/kerosene, Desal. Wat. Treat., 54 (2015) 191–199.
[34] E. Bringas, M.F.S. Roman, J.A. Irabien, I. Ortiz, An overview of the mathematical modelling of liquid membrane separation processes in hollow fibre contactors, J. Chem. Technol. Biotechnol., 84 (2009) 1583–1614.
[35] A.M. Urtiaga, J.A. Irabien, Internal mass-transfer in hollow fiber supported liquid membranes, AIChE J., 39 (1993) 521–525.
[36] F.I. Alguacil, M. Alonso, F.A. Lopez, A. Lopez-Delgado, I. Padilla, Dispersion-free solvent extraction of Cr(VI) from acidic solutions using hollow fiber contactor, Environ. Sci. Technol., 43 (2009) 7718–7722.
[37] A. Kumar, A.M. Sastre, Hollow fibre supported liquid membrane for the separation/concentration of gold(I) from aqueous cyanide media: modelling and mass transfer evaluation, Ind. Eng. Chem. Res., 39 (2000) 146–154.
[38] Y.X. Li, C.W. Cui, Extraction behavior of Cr(VI) and coexistence with interfering ions by trialkylamine, J. Water Reuse Desal., 5 (2015) 494–504.